



# EFFICIENT DETERMINATION OF MECHANICAL PROPERTIES OF CARBON FIBRE-REINFORCED LAMINATED COMPOSITE PANELS

Umar Farooq and Peter Myler

Faculty of Engineering and Advanced Sciences, University of Bolton BL3 5AB, United Kingdom

E-Mail: [adalzai3@yahoo.co.uk](mailto:adalzai3@yahoo.co.uk)

## ABSTRACT

This paper is concerned with integrating experimental and theoretical methods supported by numerical simulations to efficiently determine mechanical properties of carbon fibre-reinforced laminated composite panels. Ignition loss experiments were conducted for eight, sixteen, and twenty-four ply laminates to approximate fibre volume fractions by weights. Rule of mixture was utilised to approximate basic mechanical properties (Young's and shear moduli and Poisson's ratios) for a lamina. The mechanical properties were utilised to develop coefficients of stiffness and compliance matrices. The coefficient matrices are used in constitutive equations to align off-axis fibres and applied load to mid-plane direction in two-dimensional formulations. Based on the two-dimensional formulations stacking sequences of three-dimensional laminate layups were developed without resorting to three-dimensional micro-macro mechanics. The formulations laminates were then coded in commercial software MATLAB<sup>TM</sup> to predict mechanical properties. Tensile and flexural physical tests of the laminates were also conducted to validate the simulation obtained mechanical properties. Comparisons of mechanical properties have shown good agreement (over 90%) between laminates having different types of stacking sequences. Based on comparison of the results an efficient and systematic two-dimensional methodology is proposed to predict mechanical properties of three-dimensional laminates.

**Keywords:** A. composite laminates, B. mechanical properties, C. tensile test, D. bending test.

## 1. INTRODUCTION

The fibre-reinforced composite laminates are being increasingly used in structural design as a building block of modern commercial aircrafts parts due to their high specific strength, high specific stiffness, light weight, and superior in-plane properties [1] and [2]. When a material is characterised experimentally, engineering constants are measured instead of the stiffness or the compliance. This is because engineering constants can be easily defined and interpreted in terms of simple state of stress and strain used in design development and analysis. Mechanical properties of the test standard laminates are obtained from static testing before using them as a structural component. But laminates are anisotropic in nature and have to undergo series of experiments to obtain their properties. Moreover, parts have certain characteristics of shape, rigidity, and strength hence their testing could be complicated [3]. Knowledge of mechanical properties to evaluate their performance and identify load bearing parameters that influence strength and response of laminates (fibre, matrix and interfaces) require efficient techniques [4]. In the literature common existing experimental methods consist of: tensile, compression, flexural, shear modulus, Iosipescu, and v-notch-rail prevail. Most of the methods are detailed in (ASTM: D7264). A large number of factors affect property determination of laminates such as: dispersion and distribution of matrix and filler, compatibility, nature, and material processing technology [5] and [6]. Hence series of tests are conducted for screening the properties before their integration in full scale structures or putting them into work. At the same time, physical testing of laminates is very inconvenient and resource consuming. Interfacial structural element and morphology also affect quality of the evaluated mechanical properties [7] and [8].

Thus larger span-to-depth ratios are used to reduce the adverse influence of the interfaces [9] and [10]. Many experimental test methods use different geometries and holding-fixtures for laminates that produce different data. Influence of shear effects in the displacements is another important factor [11] and [12]. The laminates subjected to off-axis loading system present tensile-shear interactions in its plies. The tensile-shear interactions lead to distortions and local micro-structural damage and failure, so in order to obtain equal stiffness in all off-axis loading systems, a composite laminate have to be balanced angle plies [13]. Some of the studies complement physical testing by using Rule of Mixture (ROM). The method could be useful approximate laminates with aligned reinforcement (stiff along the fibres) and very weak (transverse to the fibres direction). Furthermore, the ROM method relates material properties of the laminates into algebraic set of equations that are easier to code and solve using computer [14]. Still use of the method is limited for cases of tensile-shear interaction if the off-axis loading system does not coincide with the main axes of a single lamina or if the laminate is not balanced [15]. The solution to obtain equal stiffness of laminates subjected in all directions within a plane is presented by various authors by stacking and bonding together plies with different fibres orientations [16] and [17]. The allocation of the appropriate input engineering parameters such as the effective elastic moduli and the associated Poisson's Ratios for the materials based on the theory of linear elasticity and their limitations are described in [18]. Theoretical approach to compute the elastic constants of laminates based on epoxy resin reinforced alternatively with glass, HM carbon, HS carbon and Kevlar49 fibres are reported in [19] and [20]. The laminates taken into account the plies sequence [0/45/90/-45/0] in order to obtain equal



stiffness in all loading systems subjected to off-axis loading systems. The elastic constants were also determined for laminates have to present balanced angle plies [21].

Review of the literature revealed that most of the existing studies are experimental where many test methods have limitations with testing and data logging systems. Majority of the analytical studies are based on ROM methods and limited to simplified two-dimensional formulation.

In the present study, effective mechanical properties for three-dimensional laminates were approximated utilising two-dimensional laminated plate theory. Quantities of volume fractions by weight were determined with ignition loss method. The volume fractions were utilised in ROM relations to approximate basic mechanical properties. The mechanical properties were utilised in laminated plate formulation to include load-deformation influence. The formulation was then coded in MATLAB<sup>TM</sup> to approximate the mechanical properties. Tensile and flexural tests were also conducted to compare and validate the results. Comparisons of experimental and simulation results were found within acceptable agreement. The study demonstrated that two-

dimensional laminated plate formulation can be systematically and effectively utilised to evaluate a range of engineering constants of three-dimensional laminates.

## 2. MATERIAL AND METHODS

### 2.1 Geometric properties of the laminates

Composites are heterogeneous materials hence full characterisation of their properties is difficult as various processing factors can influence the properties such as misaligned fibres, fibre damage, non-uniform curing, cracks, voids and residual stresses. These factors are assumed to be negligible when care is taken in the manufacturing process. It is for this reason that the purpose specific aerospace specialist fabricated laminates (manufacturers' supplied) were used here. For a better understanding of the laminate, a brief illustration of the coordinate systems used is shown in Figure-1. The X-Y-Z system is the global coordinates system. The 1-2-3 system is the local material coordinates system defined for each ply with the 1 axis representing the fibre direction, the 2 axis representing the direction perpendicular to the fibre direction and the 3 axis representing the out-of-plane direction.

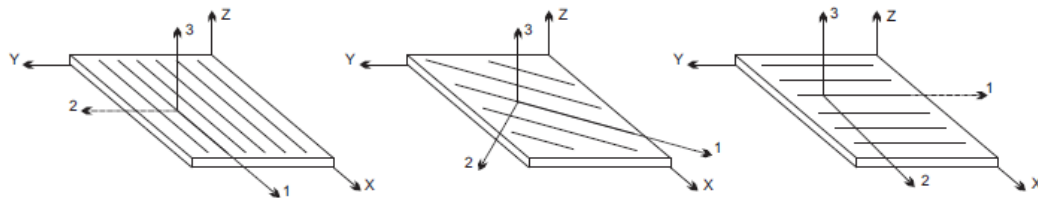


Figure-1. Coordinate systems convention.

A typical 8-Ply laminate is shown in Figure-2.

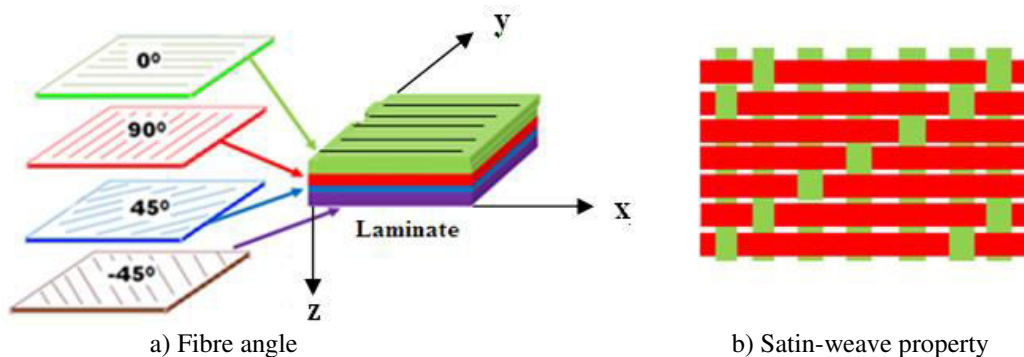


Figure-2. Schematic of 8-Ply symmetric laminate.

The laminates are also assumed to be void-free, linear elastic with plane dimensions 150mm x 120mm with fibre horns technique of every fourth layer. Average

thicknesses of the laminates consisting of eight-, sixteen-, and twenty-four plies with layup sequence are given in Table-1.

**Table-1.** Measured thickness of laminates.

Laminates	Code: Fibredux 914C-833-40	
No. of ply	Lay-up code	Average thickness mm
8	[0/90/45/-45] <sub>S</sub>	2.4
16	[0/90/45/-45] <sub>2S</sub>	4.8
24	[0/90/45/-45] <sub>3S</sub>	7.2

The material properties are given in Table-2.

**Table-2.** Material properties of the laminates.

Property parameters	Units	Fibredux 914C-833-40
Tensile Modulus $E_{xx}$ , $E_{yy}$ in $0^\circ$ & $90^\circ$ and in $45^\circ$ & $-45^\circ$	Gpa	230
Shear Modulus $G_{12}$	Gpa	88
Poisson's Ratio ( $\nu_{12}$ )		0.21

## 2.2 Volume fractions obtained from ignition loss method

Densities of fibres and resin–matrix contents were determined experimentally by weighing them in air. The ignition loss method (ASTM: D2854-68) was used for polymeric matrix composites containing fibres that do not lose weight at high temperature. In this method, cured resin is burnt off from a small test at  $585^\circ\text{C}$  in a muffle furnace. After burning for three hours at  $585^\circ\text{C}$  the density of fibres comes down to  $1.8\text{g/cm}^3$  and that of the matrix as  $2.09\text{g/cm}^3$ . Three laminates were tested and fibre percentages (residue mass/sample mass) per unit volume ( $\text{cm}^3$ ) were calculated as shown in Table-3 given below. The density quantities shown in column 7 were then utilised in 'Rule of Mixture' to calculate volume fraction of carbon fibres as shown in column 8 of the same Table.

**Table-3.** Fibre contents of laminates.

Sample	Heated up to $585^\circ\text{C}$						
	Length	Width	Depth	Sample mass g	Residue mass g	Density $\text{g/cm}^3$	Carbon fibre %
8-Ply	22.40	2.13	5.89	0.4434	0.17	1.779	50.7
16-Ply	13.4	5.84	11.56	1.4555	0.7396	1.816	50.8
16-Ply	12.61	5.75	11.47	1.3924	0.7027	1.786	50.5

## 3. METHODOLOGY TO DETERMINE MECHANICAL PROPERTIES

Conventions used in this study:

- Elastic constants are expressed throughout in normal format rather than italic to keep uniformity with the other variables in equations.
- Micromechanics does not refer to mechanical behavior at the molecular level rather it looks at components of a composite (matrix and fibre) and tries to predict the behavior of the assumed homogeneous composite material.
- The behavior of the lamina is called "macro-mechanics". Most of the structural parts use laminates that consist of several plies with different orientations connected together through a bonding interface.

### 3.1 Micro-mechanics methods

A lamina (heterogeneous at the constituent level) forms the building block of laminated composites based structures. The mechanical and physical properties of the laminae (reinforcement and matrix) and their interactions are examined on a microscopic level on various degrees of simplifications. Fibre and matrix densities are measured and converted into respective fibre volume fractions that form basis for approximation of engineering properties (see Figure-3).



## Micromechanics



## Macromechanics

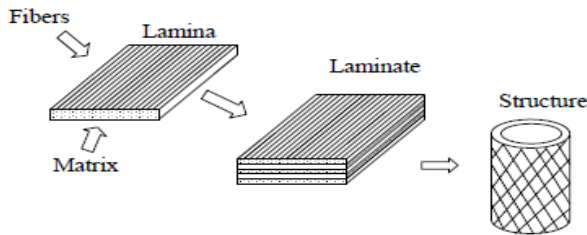


**Figure-3.** Micro and macro-mechanics process for property determination.

The measured densities and fibre volume fractions of a laminate can be related to its ingredients using 'Rule of Mixture' and utilised to determine volume fractions by weight. The volume and weight fractions are given in Eq. (1) and Eq. (2) below:

$$V_c = V_f + V_m + V_v = 1 = \text{composite volume} \quad (1)$$

Where:  $V_f = \frac{V_f}{V_c}$  = fibre volume fraction;  $V_m = \frac{V_m}{V_c}$  = matrix volume fraction; and  $V_v = \frac{V_v}{V_c}$  = void volume fraction

The weight fractions are given with the relation:

$$W_c = W_f + W_m = \text{composite weight (void weight is neglected)} \quad (2)$$

Where:  $W_f = \frac{W_f}{W_c}$  = fibre weight fraction and  $W_m = \frac{W_m}{W_c}$  = matrix weight fraction

The density ( $\rho = \frac{W}{V}$ ) is used to approximate volume fractions = density

$$\rho_c = \frac{1}{\frac{W_f}{\rho_f} + \frac{W_m}{\rho_m}} \quad (3)$$

$$\frac{W_c}{\rho_c} = \frac{W_f}{\rho_f} + \frac{W_c - W_f}{\rho_m} \quad (4)$$

$$1 = \frac{\left(\frac{W_f}{\rho_f}\right) + \left(\frac{W_c - W_f}{\rho_m}\right)}{\frac{W_c}{\rho_c}} \quad (5)$$

$$\rho_c V_c = \rho_f V_f + \rho_m V_m \text{ (Rule of mixture for density)} \quad (6)$$

Eq. (1) can be rearranged as

$$V_c = 1 - \frac{\left(\frac{W_f}{\rho_f}\right) + \left(\frac{W_c - W_f}{\rho_m}\right)}{\frac{W_c}{\rho_c}} \quad (7)$$

Where:

The symbols W, V, and  $\rho$  represent weight, volume, and density. The subscripts c, f, m, and v denote composite, fibre, matrix, and void, respectively.

Fibre volume fraction from densities neglecting void contents zero is:

$$FVF = \frac{(\rho_c - \rho_m)}{(\rho_f - \rho_m)} \quad (8)$$

The fibre volume fraction from fibre weight fraction

$$FVF = \left[1 + \frac{\rho_f}{\rho_m} \left(\frac{1}{FWF} - 1\right)\right]^{-1} \quad (9)$$

Where

$$FWF = \frac{\rho_f FVF}{\rho_m + ((\rho_f - \rho_m) \cdot FVF)} \quad (10)$$

The cured ply thickness from ply weight ([www.gurit.com](http://www.gurit.com)):

$$CPT_{(mm)} = \frac{W_F}{1000 \rho_f FVF} \quad (11)$$

Where:

FVF = fibre volume fraction  
FWF = fibre weight fraction  
 $\rho_c$  = density of composite ( $\text{g/cm}^3$ )  
 $\rho_m$  = density of cured resin/hardener matrix ( $\text{g/cm}^3$ )  
 $\rho_f$  = density of fibres ( $\text{g/cm}^3$ )  
 $W_F$  = fibre area weight of each ply ( $\text{g/m}^2$ )  
CPT (mm) = Cured ply thickness calculated from volume fraction.

From the Eq. (9) and Eq. (10) fibre volume fraction by weight was determined as 54% using MATLAB<sup>TM</sup> code Figure-4.



```
% Computing values from mat lab
% Effective Length = Length 120 mm – Grips 30 mm = 90 mm
l=90;b=23; delta=0.4;
ply=input('enter no of ply');
if(ply==8)% p is applied load
p=25; h=2.4;
elseif (ply==16)
p=190; h=4.8
else (ply==24)
p=600;h=7.2;
end
mom=p*l/2; i= 23*(h^3)/12; smax=(mom*(h/2))/i; elast=(p*l^3)/(48*delta*i); epsi=smax/elast;
disp(mom);disp(i);disp(smax);disp(elast);disp(epsi)
% Values computed from Matlab software for sample D
% Average length
l1= 12.84;l2=12.38;l=(l1+l2)/2;
%Average width
w1= 11.4;w2=11.54;w=(w1+w2)/2;
%Average thickness
t1= 6.84;t2=4.68;t=t1+t2;
% Volume of sample D
volume = l*w*t;
disp('volume of the sample is'); disp(volume);
% sample mass and density
smass = 0.3672;denst1=smass/volume;
disp('density of the sample is'); disp(denst1);
% Residue mass and density
residu = 0.1666; rmass = 0.1666; denst2 = rmass/volume;
disp('density of the residue is ');disp(denst2)
% Calculations for volume and weight fibre fractions
imass = 1.3924; % initial mass fmass = 0.7027; % final mass
ratio1=fmass/imass; ratio1= 1/ratio1; ratio1=1-ratio1
% values found from the Internet
rowf = 1.8; % fibre density rowm = 2.09; % matrix density
ratio2=rowf/rowm; denom1 = ratio1*ratio2; denom1 = denom1+1;
fvf = 1/denom1;
disp(fvf)= 0.5419
% fibre weight fraction from fibre volume fraction
rowf= 1.8;rowm=2.09;fvf = 0.5419;
denom1 = rowm+(rowf-rowm)*fvf;fwf=rowf*fvf/denom1;
disp(fwf)
=0.5207
```

Figure-4. MATLAB™ code to compute volume fractions by weight.

### 3.1.1 Mechanical properties of a lamina

By the rule of mixtures, the modulus of a composite is defined as the combination of the modulus of the fibre and the modulus of the matrix that are related to the volume fractions of the constituent materials [11]:

$$E_c = E_f V_f + E_m V_m \quad (12)$$

Where:  $E_c$  is the modulus of elasticity of the composite Assuming perfect bonding very small modulus of matrix, the equations for calculating ply moduli are written as:

$$E_1 = E_f V_f + E_m V_m \text{ (Longitudinal Young's modulus)} \quad (13)$$

$$E_2 = \frac{E_m V_f + E_f V_m}{E_m E_f} \text{ (Transverse Young's modulus)} \quad (14)$$

$$G_{12} = \frac{G_f G_m}{G_m V_f + G_f V_m} \text{ (In-plane shear modulus)} \quad (15)$$

$$\nu_{12} = \nu_f V_f + \nu_m V_m \text{ (Poisson's ratios)} \quad (16)$$

### 3.2.1 Determination of critical volume fractions

Fibre volume fraction using Eq. (9) and Eq. (10) can be re-written as:

$$V_f = \frac{W_f}{\rho_f} \left[ \left( \frac{W_f}{\rho_f} + (1 - W_f) \rho_m \right) \right]^{-1} \quad (17)$$



$$\rho_c = 1x \left[ \left( \frac{W_f}{\rho_f} + (1 - W_f) \right) \rho_m \right]^{-1} \quad (18)$$

In terms of fibre volume fraction,  $V_f$ , the composite density,  $\rho_c$ , can be written as

$$\rho_c = \rho_f V_f + \rho_m (1 - V_f) \quad (19)$$

From the assumption of perfect bonding between fibres and matrix, we can write:

$$\varepsilon_f = \varepsilon_m = \varepsilon_c \quad (20)$$

Since both fibres and matrix are elastic, the representative longitudinal systems can be calculated as

$$\sigma_f = E_f \varepsilon_f = E_f \varepsilon_c \quad (21)$$

$$\sigma_m = E_m \varepsilon_m = E_m \varepsilon_c \quad (22)$$

Comparing Eq. (21) and Eq. (22) and knowing from material properties that  $E_f \gg E_m$  we conclude that the fibre stress  $\sigma_f > \sigma_m$ . The total tensile load  $P$  applied on the composite lamina is shared by fibres and matrix so that

$$P = P_f + P_m \quad (23)$$

Equation (23) can be written as  $\sigma_c A_c = \sigma_f A_f + \sigma_m A_m$  (24)

or

$$\sigma_c = \sigma_f \frac{A_f}{A_c} + \sigma_m \frac{A_m}{A_c} \quad (25)$$

Since  $V_f = \frac{A_f}{A_c}$  and  $V_m = \frac{A_m}{A_c}$ , the Eq. (25) gives

$$\sigma_c = \sigma_f V_f + \sigma_m V_m \quad (26)$$

$$= \sigma_f V_f + \sigma_m (1 - V_f) \quad (27)$$

Dividing both sides of the Eq. (27) by  $\varepsilon_c$  and using Eq. (21) & (22), we can write the longitudinal modulus for the composites as

$$E_1 = E_f V_f + E_m (1 - V_f) \quad (28)$$

Equation (28) is called the rule of mixture that shows that the composite's longitudinal modulus is intermediate between fibre and matrix moduli. The fraction of load carried by fibres in a unidirectional continuous fibre lamina is

$$\begin{aligned} \frac{P_f}{P} &= \sigma_f V_f [\sigma_f V_f + \sigma_m (1 - V_f)]^{-1} \\ &= E_f V_f [E_f V_f + E_m (1 - V_f)]^{-1} \end{aligned} \quad (29)$$

In general, fibre failure strain is lower than the matrix failure strain. Assuming all fibres have the same strength, the tensile rupture of fibres will determine the rupture in the composite. In polymeric matrix composite is  $\frac{E_f}{E_m} > 10$ . Thus, even for  $V_f = 0.2$ , fibres carry more than 70% of composite load. Thus, using Eq. (28), the longitudinal tensile strength  $\sigma_{Ltu}$  of a unidirectional continuous fibre can be estimated as

$$\sigma_{Ltu} = \sigma_{fu} V_f + \sigma_{mu} (1 - V_f) \quad (30)$$

Where:  $\sigma_{fu}$  is fibre tensile strength;  $\sigma_{mu}$  is matrix stress at fibre failure strain ( $\varepsilon_m = \varepsilon_{fu}$ ).

For effective measurement of the reinforcement of the matrix ( $\sigma_{Ltu} \geq \sigma_{mus}$ ), the fibre volume fraction in the composite must be greater than a critical value. This critical volume fraction is calculated by setting  $\sigma_{Ltu} = \sigma_{mus}$ . Thus, from Eq. (30), the value can be calculated as:

$$V_{f\_Critical} = [\sigma_{mus} - \sigma_{mu}] [\sigma_{fu} - \sigma_{mus}]^{-1} \quad (31)$$

The fibre weight fraction was computed as 50% using the computer code given in Figure-4 agrees with the major requirement of the acceptable range of ( $\pm 5\%$ ) fibre contents to determine elastic constants before using them in the investigation.

### 3.1.3 Formulations for coefficients of stiffness and compliance matrices

The relationships of composite material properties, relative volume contents, and geometric arrangement of the constituent materials are useful in mechanics of materials models. Engineering constants measured from rule of mixture are used to determine components of lamina the stiffness matrix  $[Q]$  and compliance matrix  $[Q]^{-1}$  from Eq. (13)-(16):

$$\begin{aligned} Q_{11} &= \frac{E_1}{1 - \nu_{12}\nu_{21}} \\ Q_{12} &= \frac{\nu_{12}E_2}{1 - \nu_{12}\nu_{21}} = \frac{\nu_{21}E_1}{1 - \nu_{12}\nu_{21}} = Q_{13} \\ Q_{22} &= \frac{E_2}{1 - \nu_{12}\nu_{21}} \\ Q_{44} &= G_{23} \\ Q_{55} &= G_{13} = G_{13} = Q_{66} \\ Q_{23} &= \frac{\nu_{23}E_2}{1 - \nu_{23}\nu_{23}} = \frac{\nu_{32}E_3}{1 - \nu_{33}\nu_{33}} \end{aligned} \quad (32)$$

The five engineering constants in stiffness/compliance matrices are very useful in the analyses of laminates having multiple laminae in non-principal coordinates. Simple relationships of transformation of stress components between coordinate local-global axes for the wedged-shape differential element can be applied to the equations of static equilibrium of loaded laminates.





### 3.2 Macro-mechanics methods

#### 3.2.1 Formulations for orthotropic lamina

The 'macro-mechanical' stress-strain relations of the lamina can be expressed in terms of an equivalent homogeneous material. However, the properties of the composites are usually anisotropic. In the angle-ply laminates the principal directions of the orthotropy of each individual ply do not coincide with the generalised coordinate system. Components of the lamina stiffness matrix need to be transformed into a global form with different angles. A unidirectional composite has three mutually orthogonal planes of material property symmetry (i.e., the 12, 23, and 13 planes) and is the orthotropic material. The 123 coordinates are referred as the principal material coordinates since they are associated with reinforcement directions. The lamina is in a two-dimensional state of stress (plane stress). The stress-strain relationships can be simplified by letting out-of-plane shear stresses zero ( $\sigma_{zz} = \tau_{xz} = \tau_{yz} = 0$ ) of a thin elastic lamina. The elastic constants influence from in-plane deformations have strain-stress relationships as:

$$\begin{aligned}\varepsilon_{xx} &= \frac{1}{E}(\sigma_{xx} - \nu\sigma_{yy}) \\ \varepsilon_{yy} &= \frac{1}{E}(-\nu\sigma_{xx} + \sigma_{yy}) \\ \gamma_{xy} &= \frac{1}{G}(\tau_{xy})\end{aligned}\quad (33)$$

Stresses in the xy-coordinate system can be transformed for an orthotropic lamina using the local-global coordinate transformation matrix:

$$\begin{Bmatrix} \sigma_1 \\ \sigma_2 \\ \tau_{12} \end{Bmatrix} = [T] \begin{Bmatrix} \sigma_x \\ \sigma_y \\ \tau_{xy} \end{Bmatrix}\quad (34)$$

$$\text{Where: } [T] = \begin{bmatrix} m^2 & n^2 & 2mn \\ n^2 & m^2 & -2mn \\ -mn & mn & m^2 - n^2 \end{bmatrix}; \quad m = \cos \theta \text{ and } n = \sin \theta$$

The elastic constants ( $E_{xx}E_{yy}\nu_{xy}$  and  $\nu_{yx}$ ) in global coordinates may be determined to relate properties of a lamina in which continuous fibres are aligned at angle  $\theta$  as shown in Figure-5.

$$\frac{1}{E_{xx}} = \frac{\cos^4 \theta}{E_{11}} + \frac{\sin^4 \theta}{E_{22}} + \frac{1}{4} \left[ \frac{1}{G_{12}} - 2 \frac{\nu_{12}}{E_{11}} \right] \sin^2 2\theta \quad (35)$$

$$\frac{1}{E_{yy}} = \frac{\sin^4 \theta}{E_{11}} + \frac{\cos^4 \theta}{E_{22}} + \frac{1}{4} \left[ \frac{1}{G_{12}} - 2 \frac{\nu_{12}}{E_{11}} \right] \sin^2 2\theta \quad (36)$$

$$\frac{1}{G_{xy}} = \frac{1}{E_{11}} + \frac{2\nu_{12}}{E_{11}} + \frac{1}{E_{22}} - \left( \frac{1}{E_{11}} + \frac{2\nu_{12}}{E_{11}} + \frac{1}{E_{22}} - \frac{1}{G_{12}} \right) \cos^2 2\theta \quad (37)$$

$$\nu_{yx} = E_{xx} \left[ \frac{\nu_{12}}{E_{11}} - \frac{1}{4} \left( \frac{1}{E_{11}} + \frac{2\nu_{12}}{E_{11}} + \frac{1}{E_{22}} - \frac{1}{G_{12}} \right) \sin^2 2\theta \right] \quad (38)$$

$$\nu_{yx} = \frac{E_{yy}}{E_{xx}} \nu_{xy} \quad (39)$$

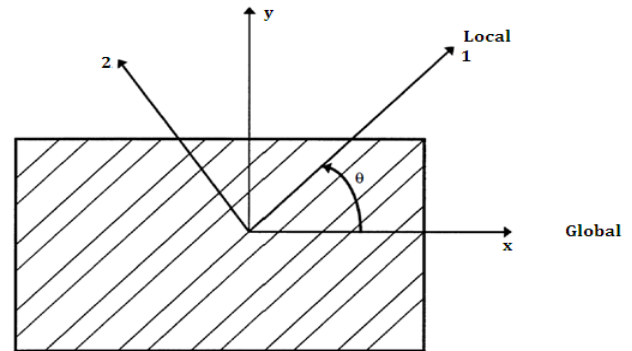


Figure-5. Unidirectional lamina reinforced with rotated fibres.

There is no coupling between the shear stresses and normal stress for an orthotropic. The strain-stress relations for a lamina in a plane stress form become:

$$\begin{aligned}\varepsilon_{xx} &= \frac{\sigma_{xx}}{E_{xx}} - \nu_{yx} \frac{\sigma_{yy}}{E_{yy}} - m_x \tau_{xy} \\ \varepsilon_{yy} &= -\nu_{xy} \frac{\sigma_{xx}}{E_{xx}} + \frac{\sigma_{yy}}{E_{yy}} - m_y \tau_{xy} \\ \gamma_{xy} &= -m_x \sigma_{xx} - m_y \sigma_{yy} + \frac{\tau_{xy}}{G_{xy}}\end{aligned}\quad (40)$$

Coefficients of mutual influence ( $m_x$  and  $m_y$ ) for an angle-lamina in global coordinates can be determined from the equations:

$$m_x = (\sin 2\theta) \left[ \frac{\nu_{12}}{E_{11}} + \frac{1}{E_{22}} - \frac{1}{2G_{12}} - (\cos^2 \theta) \left( \frac{1}{E_{11}} + \frac{2\nu_{12}}{E_{11}} + \frac{1}{E_{22}} - \frac{1}{G_{12}} \right) \right] \quad (41)$$

$$m_y = (\sin 2\theta) \left[ \frac{\nu_{12}}{E_{11}} + \frac{1}{E_{22}} - \frac{1}{2G_{12}} - (\sin^2 \theta) \left( \frac{1}{E_{11}} + \frac{2\nu_{12}}{E_{11}} + \frac{1}{E_{22}} - \frac{1}{G_{12}} \right) \right] \quad (42)$$

The symmetry presented by the unidirectional lamina makes it so-called orthotropic material. For an especially orthotropic lamina ( $\theta = 0^\circ$  and  $90^\circ$ ), the stress-strain relations yield:

$$\begin{aligned}\varepsilon_{xx} &= \varepsilon_{11} = \frac{\sigma_{xx}}{E_{11}} - \nu_{21} \frac{\sigma_{yy}}{E_{22}} \\ \varepsilon_{yy} &= \varepsilon_{22} = -\nu_{12} \frac{\sigma_{xx}}{E_{11}} + \frac{\sigma_{yy}}{E_{22}} \\ \gamma_{xy} &= \gamma_{yx} = \gamma_{12} = \gamma_{21} = \frac{\tau_{xy}}{G_{xy}}\end{aligned}\quad (43)$$

Using Eq. (32), the relations may be written in local coordinates as:

$$\begin{Bmatrix} \sigma_1 \\ \sigma_2 \\ \tau_{12} \end{Bmatrix} = \begin{bmatrix} Q_{11} & Q_{12} & 0 \\ Q_{12} & Q_{22} & 0 \\ 0 & 0 & Q_{66} \end{bmatrix} \begin{Bmatrix} \varepsilon_1 \\ \varepsilon_2 \\ \gamma_{12} \end{Bmatrix} \quad (44)$$



Similarly, for the general orthotropic lamina ( $\theta \neq 0^\circ$  and  $90^\circ$ ), the complete set of transformation equations for the stresses in the xy-coordinate system can be developed using the local-global coordinate transformation matrix. The generally orthotropic laminate creates fully populated, the reduced transformed stiffness matrix:

$$\begin{Bmatrix} \sigma_x \\ \sigma_y \\ \tau_{xy} \end{Bmatrix} = \begin{bmatrix} \bar{Q}_{11} & \bar{Q}_{12} & \bar{Q}_{16} \\ \bar{Q}_{12} & \bar{Q}_{22} & \bar{Q}_{26} \\ \bar{Q}_{16} & \bar{Q}_{26} & \bar{Q}_{66} \end{bmatrix} \begin{Bmatrix} \varepsilon_x \\ \varepsilon_y \\ \gamma_{xy} \end{Bmatrix} \quad (45)$$

Where matrices:  $[\bar{Q}] = [T]^{-1}[Q][R][T][R]^{-1}$  and Reuter transforms

$[R] = \begin{bmatrix} 1 & 0 & 0 \\ 0 & 1 & 0 \\ 0 & 0 & 2 \end{bmatrix}$  for strains can be performed in the same manner using tensor strain as engineering shear strain. It is not a tensor quantity and is twice the tensor shear strain ( $\gamma_{12} = 2\varepsilon_{12}$ ).

The models given in Eq. (45) are complicated hence semi-empirical models have been developed for the design purposes. They can be used over a wide range of elastic properties and fibre volume fractions. The equations are semi-empirical in nature since involved parameters in the curve fitting carry physical meaning. The sharp drop in modulus as the angle changes slightly from  $0^\circ$  is its limitation since over much of the range of lamina orientation the modulus is very low which requires transverse reinforcement in most composites. The shear-coupling effects are the generation of shear strains by off-axis normal stresses and the generation of normal strains by off-axes shear stresses. The degree of shear coupling is defined by dimensionless shear-coupling ratios or mutual influence coefficients or shear-coupling coefficients. The mutual influence coefficients can be found from:

$$\eta_{x,xy} = \frac{\gamma_{xy}}{\varepsilon_{xx}} \quad (46)$$

Similarly, when the state of stress is defined as  $\sigma_{yy} \neq 0, \sigma_{xx} = \tau_{xy} = 0$ , the ratio

$$\eta_{y,xy} = \frac{\gamma_{xy}}{\varepsilon_{yy}} \quad (47)$$

Pure shear stresses  $\tau_{xy} \neq 0, \sigma_{xx} = \sigma_{yy} = 0$ , the ratio  $\eta_{xy,y}$  characterises the normal strain response along the y direction due to a shear stress in the x-y plane. The ratio can be found as:

$$\eta_{xy,y} = \frac{\tau_{xy}}{G_{xy}} \quad (48)$$

Superposition of loading, stress-strain relations in terms of elastic constants are:

$$\begin{Bmatrix} \varepsilon_{xx} \\ \varepsilon_{yy} \\ \gamma_s \end{Bmatrix} = \begin{bmatrix} \frac{1}{E_{xx}} & -\frac{\nu_{yx}}{E_{yy}} & \frac{\eta_{sx}}{G_{xy}} \\ -\frac{\nu_{yx}}{E_{xx}} & \frac{1}{E_{yy}} & \frac{\eta_{sy}}{G_{xy}} \\ \frac{\eta_{sx}}{G_{xy}} & \frac{\eta_{sy}}{G_{xy}} & \frac{1}{G_{xy}} \end{bmatrix} \begin{Bmatrix} \sigma_{xx} \\ \sigma_{yy} \\ \tau_s \end{Bmatrix} \quad (49)$$

The modulus of elasticity and tensile strength of a laminate under a uniaxial load applied in the x-direction at an angle  $\theta$  to the fibres 1-direction may be determined from the transformed reduced stiffness matrix. The moduli:  $E_{xx}$ ,  $E_{yy}$ ,  $G_{xy}$ , and  $\nu_{xy}$  in global coordinates can be written as:

$$E_{xx} = \frac{1}{\left[ \frac{m^2}{E_{11}} (m^2 - n^2 \nu_{12}) + \frac{n^2}{E_{22}} (n^2 - m^2 \nu_{12}) + \frac{m^2 n^2}{G_{12}} \right]} \quad (50)$$

$$E_{yy} = \frac{1}{\left[ \frac{n^2}{E_{11}} (n^2 - m^2 \nu_{12}) + \frac{m^2}{E_{22}} (m^2 - n^2 \nu_{21}) + \frac{m^2 n^2}{G_{12}} \right]} \quad (51)$$

$$G_{xy} = \frac{1}{\left[ \frac{4m^2 n^2}{E_{11}} (1 + \nu_{12}) + \frac{4m^2 n^2}{E_{22}} (1 + \nu_{21}) + \frac{(m^2 - n^2)^2}{G_{12}} \right]} \quad (52)$$

$$\nu_{xy} = \frac{E_{xx}}{\left[ \frac{m^2}{E_{11}} (m^2 \nu_{12} - n^2) + \frac{n^2}{E_{22}} (n^2 \nu_{12} - m^2) + \frac{m^2 n^2}{G_{12}} \right]} \quad (53)$$

$$\nu_{yx} = \frac{E_{yy} \nu_{xy}}{E_{xx}} \quad (54)$$

$$\eta_{xs}/E_{xx} = \eta_{sx}/G_{xy} = \left[ \frac{2m^3 n}{E_{11}} (1 + \nu_{12}) - \frac{2mn^3}{E_{22}} (1 + \nu_{21}) - \frac{mn(m^2 - n^2)}{G_{12}} \right] \quad (55)$$

$$\eta_{ys}/E_{yy} = \eta_{sy}/G_{xy} = \left[ \frac{2mn^3}{E_{11}} (1 + \nu_{12}) - \frac{2mn^3}{E_{22}} (1 + \nu_{21}) + \frac{mn(m^2 - n^2)}{G_{12}} \right] \quad (56)$$

The Eq. (55) and (56) illustrate an angle-ply laminate in which the various plies are orientated at  $\pm \theta$  to the plate element axes, in this case the x-axis. The laminates which have an equal member of  $+\theta$  and  $-\theta$  plies are balanced about their mid-plane are orthotropic in nature. In the case stresses and strains related by the transformed reduced stiffness matrix:

$$\begin{Bmatrix} \sigma_x \\ \sigma_y \\ \sigma_z \\ \sigma_{yz} \\ \sigma_{xz} \\ \sigma_{xy} \end{Bmatrix} = \begin{bmatrix} \bar{Q}_{11} & \bar{Q}_{12} & \bar{Q}_{13} & 0 & 0 & \bar{Q}_{16} \\ \bar{Q}_{12} & \bar{Q}_{22} & \bar{Q}_{23} & 0 & 0 & \bar{Q}_{26} \\ \bar{Q}_{13} & \bar{Q}_{23} & \bar{Q}_{33} & 0 & 0 & \bar{Q}_{36} \\ 0 & 0 & 0 & \bar{Q}_{44} & 0 & 0 \\ 0 & 0 & 0 & 0 & \bar{Q}_{55} & 0 \\ \bar{Q}_{16} & \bar{Q}_{26} & \bar{Q}_{36} & 0 & 0 & \bar{Q}_{66} \end{bmatrix} \begin{Bmatrix} \varepsilon_x \\ \varepsilon_y \\ \varepsilon_z \\ \gamma_{yz} \\ \gamma_{xz} \\ \gamma_{xy} \end{Bmatrix} \quad (57)$$

The thirteen constants  $\bar{Q}_{ij}$  are related to nine  $Q_{ij}$  through the following transformation the components of the transformed stiffness matrix defined as follows:





$$\begin{aligned}
 \bar{Q}_{11} &= Q_{11}\cos^4\theta + Q_{22}\sin^4\theta + 2(Q_{12} + 2Q_{66})\sin^2\theta\cos^2\theta \\
 \bar{Q}_{12} &= (Q_{11} + Q_{22} - 4Q_{66})\sin^2\theta\cos^2\theta + Q_{12}(\cos^4\theta + \sin^4\theta) \\
 \bar{Q}_{13} &= Q_{13}\cos^2\theta + Q_{23}\sin^2\theta \\
 \bar{Q}_{22} &= Q_{11}\cos^4\theta + Q_{22}\sin^4\theta + 2(Q_{12} + 2Q_{66})\sin^2\theta\cos^2\theta \\
 \bar{Q}_{23} &= Q_{13}\sin^2\theta + Q_{23}\cos^2\theta \\
 \bar{Q}_{33} &= Q_{33} \\
 \bar{Q}_{16} &= (Q_{11} - Q_{12} - 2Q_{66})\sin\theta\cos^3\theta \\
 &\quad - (Q_{22} - Q_{12} - 2Q_{66})\cos\theta\sin^3\theta \\
 \bar{Q}_{26} &= (Q_{11} - Q_{12} - 2Q_{66})\cos\theta\sin^3\theta \\
 &\quad - (Q_{22} - Q_{12} - 2Q_{66})\sin\theta\cos^3\theta \\
 \bar{Q}_{36} &= (Q_{13} - Q_{23})\sin\theta\cos\theta \\
 \bar{Q}_{44} &= Q_{44}\cos^2\theta + Q_{55}\sin^2\theta \\
 \bar{Q}_{45} &= (Q_{45} - Q_{44})\sin\theta\cos\theta \\
 \bar{Q}_{55} &= Q_{55}\cos^2\theta + Q_{44}\sin^2\theta \\
 \bar{Q}_{66} &= (Q_{11} + Q_{22} - 2Q_{12} - 2Q_{66})\sin^2\theta\cos^2\theta + \\
 &\quad Q_{66}(\cos^4\theta + \sin^4\theta)
 \end{aligned} \quad (58)$$

Although the transformed - matrix now has the form as that of anisotropic material with nine nonzero coefficients, only four of the coefficients are independent because they can all be expressed in terms of the four independent stiffness of the specially orthotropic material. The lamina engineering constants can also be transformed from principal material axes to the off-axes coordinates. The effects of lamina orientation on stiffness are difficult to assess from inspection stiffness transformation equations. In addition, the eventual incorporation of lamina stiffness over the laminate thickness, and integration of such complicated equations is also difficult. In view of the difficulties, a more convenient form of lamina stiffness transformation equations has been proposed in [12]. By using trigonometric identities to convert from power functions to multiple angle functions and then using additional mathematical manipulations. The invariants are simply linear combinations of the  $Q_{ij}$ , are invariant to rotations in the plane of the lamina. Thus, the effects of lamina orientation on stiffness are easier to interpret. Invariant formulations of lamina compliance transformations are also orthogonal. From Eq. (29) it appears that there are six constants that govern the stress-strain behaviour of a lamina. However, the equations are linear combinations of the four basic elastic constants, and therefore are not independent. Elements in stiffness matrices can be expressed in terms of five invariant properties of the lamina using trigonometric identities in [21].

The invariants to rotations are simply linear combinations in plane of the lamina. There are four independent invariants, just as there are four independent elastic constants. In all the stiffness expressions (except coupling) consist of one constant term which varies with lamina orientations. Thus, the effects of lamina orientation on stiffness are easier to interpret very useful in computing elements of these matrices. The element of fibre-reinforced composite material with its fibre oriented at some arbitrary angle exhibits a shear strain when subjected to a normal stress, and it also exhibits an extensional strain

when subjected to a shear stress. The state of stress is defined as where  $\sigma_{xx} \neq 0, \sigma_{yy} = \tau_{xy} = 0$ .

### 3.2.2 Formulation for effective constants of laminates

The quantities of the elastic constants of every plies in material coordinates were utilised to approximate effective elastic constants for laminated structural element of thickness  $H$  made of  $N$  plies in global coordinates:

$$\bar{E}_1 = \frac{1}{HN} \sum_{i=0}^N E_1(\theta_i) \quad (59)$$

$$\bar{E}_2 = \frac{1}{HN} \sum_{i=0}^N E_2(\theta_i) \quad (60)$$

$$\bar{G}_{12} = \frac{1}{HN} \sum_{i=0}^N G_{12}(\theta_i) \quad (61)$$

$$\bar{\nu}_{12} = \frac{1}{HN} \sum_{i=0}^N \nu_{12}(\theta_i) \quad (62)$$

$$\bar{\nu}_{21} = \frac{1}{HN} \sum_{i=0}^N \nu_{21}(\theta_i) \quad (63)$$

The effective elastic constants in the x-axis direction  $E_x$ , in the y-axis direction  $E_y$ , the effective Poisson's ratios  $\nu_{xy}$  and  $\nu_{yx}$ , and the effective shear modulus in the x-y plane  $G_{xy}$  are computed. As symmetric balanced laminates were considered therefore the following three average laminate stresses were defined [1]:

$$\sigma_x = \frac{1}{H} \int_{-H/2}^{H/2} \sigma_x dz \quad (64)$$

$$\sigma_y = \frac{1}{H} \int_{-H/2}^{H/2} \sigma_y dz \quad (65)$$

$$\tau_{xy} = \frac{1}{H} \int_{-H/2}^{H/2} \tau_{xy} dz \quad (66)$$

Where:  $H$  is the thickness of the laminate. Integration through-thickness in Eq. (64)-(66) with was approximated as a summation to obtain the average stresses and related to the force resultants ( $N_x, N_y$ , and  $N_{xy}$ ) as:

$$\sigma_x = \frac{1}{H} N_x \quad (67)$$

$$\sigma_y = \frac{1}{H} N_y \quad (68)$$

$$\tau_{xy} = \frac{1}{H} N_{xy} \quad (69)$$

To relate strains to the stresses:

$$\begin{Bmatrix} \varepsilon_x^0 \\ \varepsilon_y^0 \\ \tau_{xy}^0 \end{Bmatrix} = \begin{bmatrix} a_{11}H & a_{12}H & 0 \\ a_{12}H & a_{22}H & 0 \\ 0 & 0 & a_{66}H \end{bmatrix} \begin{Bmatrix} \bar{\sigma}_x \\ \bar{\sigma}_y \\ \bar{\tau}_{xy} \end{Bmatrix} \quad (70)$$

The effective elastic constants can be obtained for the laminate using  $3 \times 3$  balanced matrix at RHS in Eq. (70):



$$\bar{E}_x = \frac{1}{a_{11}H} \quad (71)$$

$$\bar{E}_y = \frac{1}{a_{22}H} \quad (72)$$

$$\bar{G}_{xy} = \frac{1}{a_{66}H} \quad (73)$$

$$\bar{\nu}_{xy} = -\frac{a_{12}}{a_{11}} \quad (74)$$

$$\bar{\nu}_{yx} = -\frac{a_{12}}{a_{22}} \quad (75)$$

The effective Poisson's ratios  $\bar{\nu}_{xy}$  and  $\bar{\nu}_{yx}$  are inter-dependent and related by the following reciprocal relations:

$$\frac{\bar{\nu}_{xy}}{\bar{E}_x} = \frac{\bar{\nu}_{yx}}{\bar{E}_y} \quad (76)$$

Where

$$a_{11} = \frac{A_{22}}{A_{11}A_{22} - A_{12}^2} \quad (77)$$

$$a_{22} = \frac{A_{11}}{A_{11}A_{22} - A_{12}^2} \quad (78)$$

$$a_{12} = \frac{A_{12}}{A_{11}A_{22} - A_{12}^2} \quad (79)$$

$$a_{66} = \frac{1}{A_{66}} \quad (80)$$

Where:

$$A_{ij} = \sum_{k=1}^n [\bar{Q}_{ij}]_k (z_k - z_{k-1}), \quad i = 1, 2, 6; j = 1, 2, 6.$$

#### 4. NUMERICAL RESULTS AND DISCUSSION

The three-dimensional formulations (Equation (45)-(51), Equation (56)-(60), Equation (59)-(63), and Equation (71)-(75) were implemented in MATLAB™ V 7.10a code to approximate the elastic constants (see Figure-6). Input properties shown in Table-2 were assigned to the respective parameters.

```
clear
clc
%Enter input data
e11=input('Enter Ex', 'e11'); e22=input('Enter Ey', 'e22');
nu12=input('Poisson's ratio', 'nu12'); g12=input('Shear-modulus', 'g12');
laminates=input('Enter no of plies in laminate', 'd');
diary Elastic_moduli_ply8.out
Q = ReducedStiffness(e11, e22, nu12, g12)
Qbar1=Qbar(Q,0);Qbar2=Qbar(Q,90); Qbar3=Qbar(Q,45); Qbar4=Qbar(Q,-45);
Qbar5=Qbar(Q,-45); Qbar6=Qbar(Q,45);Qbar7=Qbar(Q,90);Qbar8=Qbar(Q,0);
z1=-1.2;z2=-0.9;z3=-0.6;z4=-0.3;z5=0.0;z6=0.3;z7=0.6;z8=0.9;z9=1.2;
A=zeros(3,3);
A=Amatrix(A,Qbar1,z1,z2);A=Amatrix(A,Qbar2,z2,z3);A=Amatrix(A,Qbar3,z3,z4);
A=Amatrix(A,Qbar4,z4,z5);A=Amatrix(A,Qbar5,z5,z6);A=Amatrix(A,Qbar6,z6,z7);
A=Amatrix(A,Qbar7,z7,z8);A=Amatrix(A,Qbar8,z8,z9);
a = inv(A);y = 1/(H*a(2,2));H=2.4;
Exx=Ebarx(A,H)
Eyy=Ebary(A,H)
Nu12=NUbarxy(A,H)
Gxy=Gbarxy(A,H)
diary off
function y = ReducedStiffness(E1,E2,NU12,G12)
%This function returns the reduced stiffness matrix size 3 x 3.
NU21 = NU12*E2/E1;
y = [E1/(1-NU12*NU21) NU12*E2/(1-NU12*NU21) 0 ;
    NU12*E2/(1-NU12*NU21) E2/(1-NU12*NU21) 0 ; 0 0 G12];
function y = Qbar(Q,theta)
%This function returns the transformed reducedstiffness matrix size 3 x 3.
m = cos(theta*pi/180);n = sin(theta*pi/180);
T = [m*m n*n 2*m*n ; n*n m*m -2*m*n ; -m*n m*n m*m-n*n];
Tinv = [m*m n*n -2*m*n ; n*n m*m 2*m*n ; m*n -m*n m*m-n*n];
y = Tinv*Q*T;
function y = Amatrix(A,Qbar,z1,z2)
%This function returns the matrix after the layer k with stiffness is %assembled.
for i = 1 : 3
    for j = 1 : 3
```



```

A(i,j) = A(i,j) + Qbar(i,j)*(z2-z1);
end
end
y = A;
function y = Ebarx(A,H)
%This function returns the average laminate modulus in the x-direction.
a = inv(A); y = 1/(H*a(1,1));
function y = NUbaryxy(A,H)
%This function returns the average laminate Poisson's ratio NUxy.
a = inv(A); y = -a(1,2)/a(1,1);
function y = Ebary(A,H)
%This function returns the average laminate modulus
a = inv(A); y = 1/(H*a(2,2));
function y = Gbarxy(A,H)
%This function returns the average laminate shear modulus.
a = inv(A); y = 1/(H*a(3,3));

```

**Figure-6.** MATLAB™ code to compute engineering constants.

The data obtained from the simulations were plotted against fibres rotated plies in the laminates. The plots highlight the relation between elastic constants at various angles. The code for plots of effective values of

four elastic constants as a function of orientation angle in the range:  $0 \leq \theta \leq \pi/2$  at the difference of 10 degrees is shown Figure-7.

```

clear
clc
%Enter input data
e11=input('Enter Ex', 'e11'); e22=input('Enter Ex', 'e22');
nu12=input('Poisson's ratio', 'nu12'); g12=input('Shear-modulus', 'g12');
laminate=input('Enter no of plies in laminate', 'd');
diary Elastic_Constants.out
fprintf('==== Angle and Elastic constants =====\n');
fprintf('-----\n\n');
fprintf('Angle   \tExx      \t\nu12   \tEyy   \tGxy \n');
fprintf('===== \t===== \t===== \t===== \t===== \n');
i=0;
for ii = 0:10:90
    i=i+1;
    ex1(i) = Ex(e11,e22, nu12, g12, ii);
    nuxy(i) = NUxy(e11,e22, nu12, g12, ii);
    ey2(i) = Ey(e11,e22, nu12, g12, ii);
    nuyx(i) = NUyx(e11,e22, nu12, g12, ii);
    gxy(i) = Gxy(e11,e22, nu12, g12, ii);

    fprintf('%2d \t%5.2f\t%5.2f\t%5.2f\t%5.2f\n',ii, ex1(i),nuxy(i),ey2(i), gxy(i))
    disp('Elastic constant')
    disp(ex1(ii))
    plot(ii,ex1(ii));
    xlabel('Angle, \theta (degree)');
    ylabel('E_{xx} (GPa)');
    title('Elastic modulus E_{xx} v Rotation','FontSize',14)
    plot(ii,nuxy(ii));
    xlabel('Angle, \theta (degree)');
    ylabel('\nu_{xy}');
    title('Elastic modulus \nu_{xy} v Rotation','FontSize',14);
    plot(ii,ey2(ii));
    xlabel('Angle, \theta (degree)');
    ylabel('E_{yy} (GPa)');
    title('Elastic modulus E_{yy} v Rotation','FontSize',14);
    plot(ii,gxy(ii));

```



```
xlabel('Angle, \theta (degree)');
ylabel('G_{xy}(GPa)');
title('Shear modulus G_{xy} v Rotation','FontSize',14);
diary off
```

**Figure-7.** MATLAB™ code to plot engineering constants v rotations.

Plots of the effective engineering constants of an 8-ply laminate as a function of angle orientations in the range:  $0 \leq \theta \leq \pi/2$  at the difference of 10 degrees are selected for discussion. The plot in Figure-8 illustrates quantities of Young's modulus in parallel to fibre (x-axis) directions. Variation of the curve shows maximum value around 230GPa as expected when fibres were aligned at

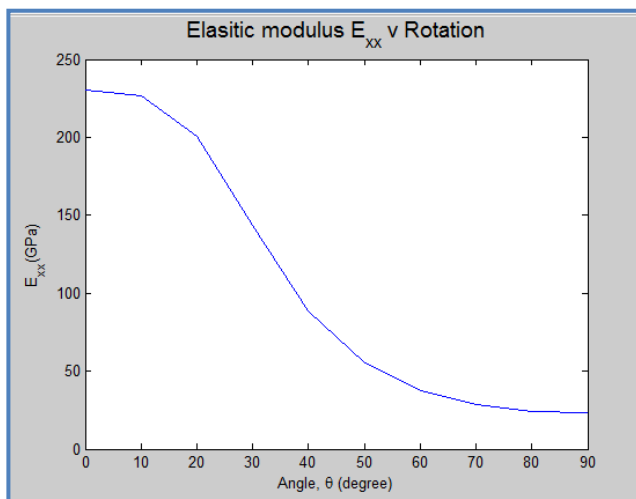
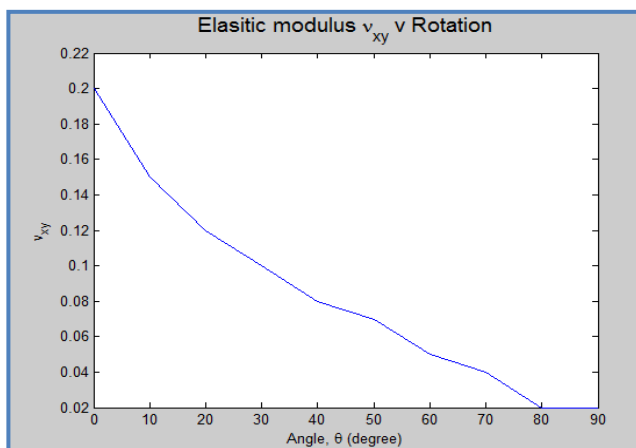


**Figure-8.** Yong's moduli in fibre direction v ply orientation.

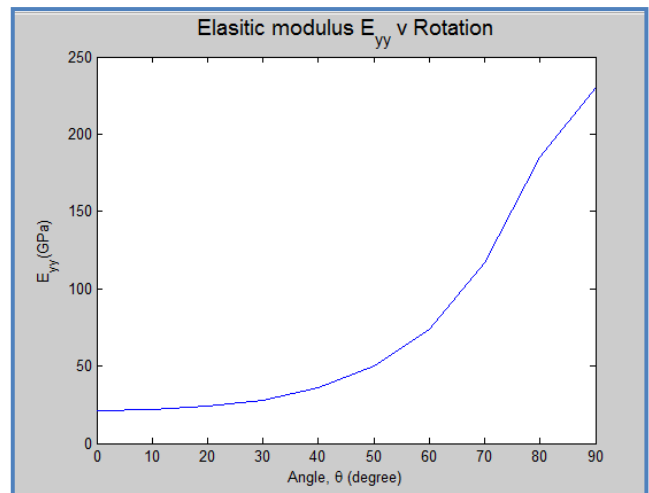
Figure-9 illustrates quantities of Poisson's ratios. Variation of the curve shows gradual drop of the values from 0.2 maximum when fibres are aligned at  $0^\circ$  rotations and minimum around 0.02 fibres were aligned at  $90^\circ$ . The curve shows decreasing trend as angle increases from  $0^\circ$  and this trend continues until angle reaches  $90^\circ$ . Changes in quantities of Young's moduli with respect to rotations support the arguments that simulations obtain values are realistic.



zero-directions. It shows severe drop as angle increases from  $0^\circ$  and this trend continues until angle reaches  $90^\circ$  where value of the modulus drops to around 23GPa. Changes in quantities of Young's moduli with respect to rotations indicate that simulation obtain values are realistic.

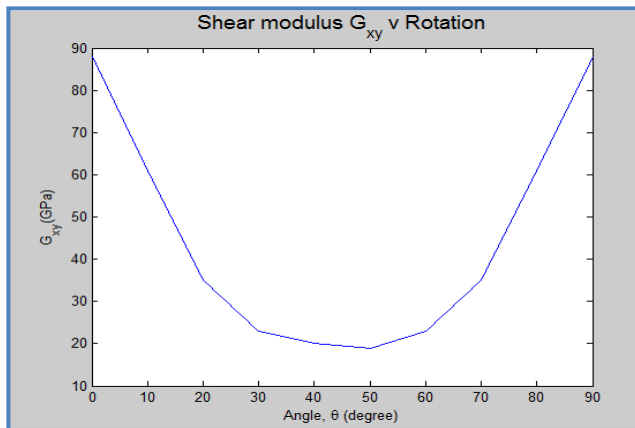
**Figure-9.** Poisson's ratios v ply orientation.

Figure-10 illustrates quantities of Young's modulus in perpendicular to fibre (y-axis) directions. Variation of the curve shows minimum value around 23GPa as expected when fibres were aligned at  $90^\circ$ . It shows increasing trend as angle increases from  $0^\circ$  and this trend continues until angle reaches  $90^\circ$  where value of the modulus reaches to around 230GPa. Changes in quantities of Poisson's ratio with respect to rotations confirm that simulation obtain values are realistic.



**Figure-10.** Young's moduli in perpendicular to fibres v ply orientation.

Figure-11 illustrates quantities of shear moduli. Variation of the curve follows parabolic path. Maximum values of 88GPa at fibre directions  $0^\circ$  can be seen which gradually to minimum around 20GPa at fibre direction  $45^\circ$  and then reverse trend begins up to  $90^\circ$  where it again reaches to 88GPa. Such types of variations were expected and that confirmed that the predicted quantities are realistic and genuine. Changes in quantities of shear-moduli with respect to rotations also confirm that simulation obtain values are realistic.



**Figure-11.** Shear modulus  $G_{xy}$  v Rotation.

Since elastic constants are interdependent hence elastic constants were computed for all the laminates. For the especially orthotropic and transversally isotropic the constants are  $G_{12}$ ,  $G_{13}$ ;  $E_2 = E_3$ ;  $\nu_{21} = \nu_{31}$ , and  $\nu_{23} = \nu_{32}$ . In addition, the relationship among the isotropic engineering constants Eq. (61) is valid associated with the 23 plane, so that  $G_{23} = \frac{E_2}{2(1+\nu_{32})}$ . Effective values for Young's moduli for all the laminates are shown in Table-4.

**Table-4.** Simulation obtained Young's moduli.

Laminate	Lay-up	Effective Young's moduli
No of ply	Code	GPa
8-Ply	[0/90/45/-45] <sub>S</sub>	56
16-Ply	[0/90/45/-45] <sub>2S</sub>	48.6
24-Ply	[0/90/45/-45] <sub>3S</sub>	45.8

## 5. VALIDATION OF SIMULATION OBTAINED ENGINEERING CONSTANTS

### 5.1 Rule of mixture

The elastic properties were calculated utilising the respective volume fractions in Eqns. (25)-(28) for 8-, 16-, and 24-Ply laminates. Identical averaged Young's moduli  $E_1$  and transverse  $E_2$  were obtained due to quasi-isotropic configuration of the laminates with fibre volume fraction for all the laminates with three different thicknesses. Quantities of the Poisson's ratios and in-plane shear-moduli also computed and good agreement of the intra-simulated values for every laminate was found. Since engineering constants are inter-dependent Young's moduli suffice the requirements. Hence Young's moduli calculated from the volume fraction equations are given in Table-5.

**Table-5.** Young's moduli computed using 'Rule of Mixture'.

Laminate	Young's modulus	Lay-up
No of ply	GPa	Code
8-Ply	58.5	[0/90/45/-45] <sub>S</sub>
16-Ply	58.6	[0/90/45/-45] <sub>2S</sub>
24-Ply	58.8	[0/90/45/-45] <sub>3S</sub>

### 5.2 Hart smith rule

The Hart Smith Rule used to calculate the elastic modulus of the laminates. The determined elastic constant for the quasi-isotropic configuration is calculated and shown in Table-6.

**Table-6.** Young's modulus determined from Hart Smith rule.

Supplied elastic modulus 230 GPa comes down to GPa for 54% contents.		
Sequence: [45/0/-45/90]	Hart Smith Rule	
Angle (degree)	Multiple	Modulus
45	.1	12.
0	1	124.
-45	.1	12.
90	.1	12.
Modulus of the 4-ply quasi-isotropic laminate		(12.+124+12+12)/4
Equivalent to the unidirectional		GPa

### 5.3 Tensile test experiment

Three laminates from each of the coupon types were prepared in I-shapes in line with the testing standard for tensile tests (ASTM: D3039). Average span and width of each laminate was 120 mm and 20 mm, respectively. Thicknesses ( $t = 2.4, 4.8$ , and  $7.2$  mm) from each of the lay-up of 8-, 16-, and 24-Ply varied due to number of plies

within the stacks. Load transfer tabs were adhesively bonded to the ends of the laminates in order that the load may be transferred from the grips of the tensile testing machine to the laminate without damaging the laminate. Laminates were gripped at both ends. Approximate dimensions and relevant spans to depth ratios are shown in Figure-12.

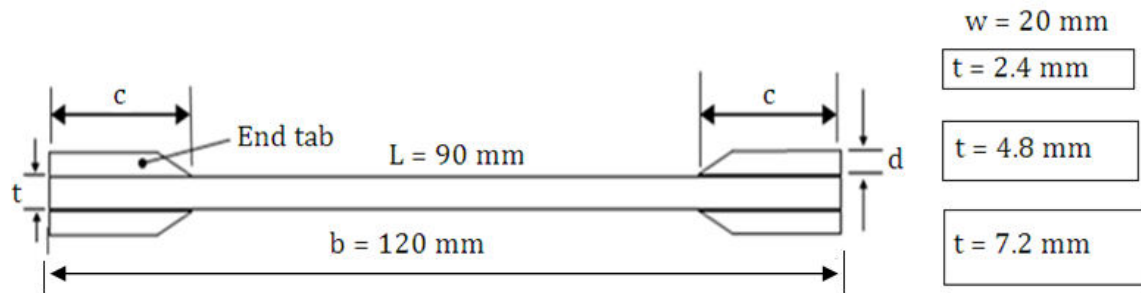


**Figure-12.** Schematic of beam laminates with cross-section.

The effective beam length (L) used for all calculations was length (120 mm) - both the grips (30 mm) = 90 mm. Average geometrical dimensions can be seen in Table-7 below.

**Table-7.** Beams lay-up configuration and geometrical dimensions.

Configuration	Grip: d	Grip: c	Thickness: t	Effective length: L
	Mm			
[45/90/0/-45] <sub>s</sub>	3	15	2.4	90
[45/90/0/-45] <sub>2s</sub>	3	15	4.8	90
[45/90/0/-45] <sub>3s</sub>	3	15	7.2	90

Photographs of the laminates selected for the tests are shown in Figure-13(a). The laminates were inserted within in the fixture holders of the machine by metal grips as shown in Figure-13(b) and loaded axially at a rate of 1mm/min. The applied tensile load produced tensile stresses through the holding grips that results elongation of the laminate in loading direction.

The applied tensile loading and corresponding voltage output values were recorded by the software installed on the data acquisition system at specified load increments so that the curve is plotted for each and every test data. Measurements for the strains were correlated from the recorded voltage ranges and scaled by the gain from the formula - given  $\varepsilon = \frac{4\Delta e}{B_v K}$ . Where:  $\Delta e$  is out-put voltage (needs to be divided by gain of 341),  $B_v$  is bridge excitation voltage (its value is: 5v), K is the gain-factor (equal to: 2.13).

Behaviour of the laminate was observed while load was being applied through variation in out-put voltage quantities during the tests of every laminate. Most of the results have shown consistency and linearity for the longitudinal strain response through system built-in display screen. A slight nonlinearity in the strain response was observed due to the influence of the matrix properties. Measurements of the strains and loads were used to determine the elastic modulus. Stresses were calculated from the applied loads on the respective areas. The recorded strains and calculated stresses were used to determine the Young's modulus as shown in Table-8. Mean moduli were calculated for the every laminate. Independent tests for every laminate were carried out for each of the laminates.

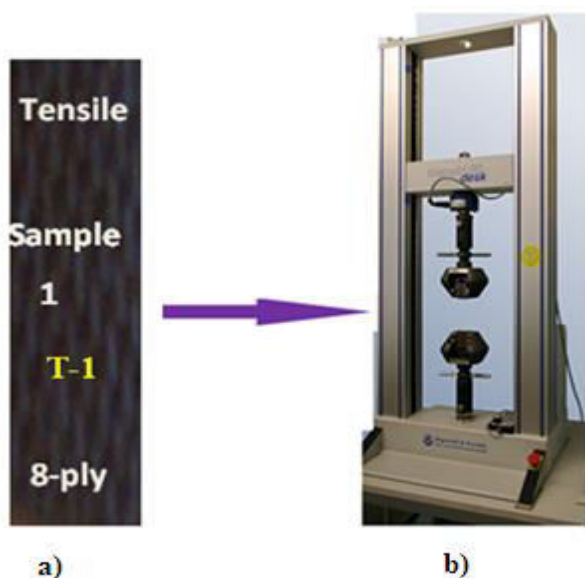


**Figure-13.** Photographs of: a) laminate and b) INSTRON™ 5585H machine.



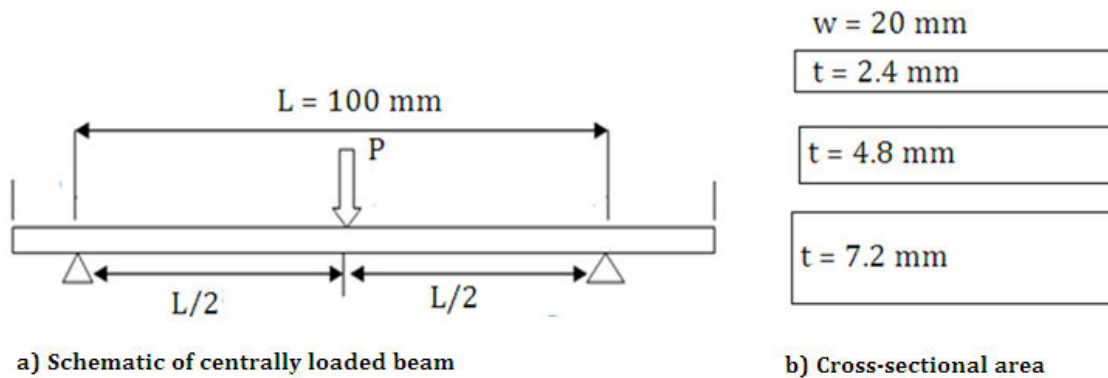
**Table-8.** Tensile test results.

Laminate		Voltage (range)	Micro- strain	Cross-sectional area mm <sup>2</sup>	Load KN	Stress GPa	Elastic modulus GPa
Test	Thickness mm						
T-1	2.4	3.14	3458	48	7.6	158.3	45.8
T-2		3.1	3414	48	7.4	154.6	45.2
T-3	4.8	2.6	2863	96	12.50	130.2	46.5
T-4		2.7	2973	96	13.	135.4	46.8
T-5	7.2	2.5	2753	144	16.	111.1	49.4
T-6		1.9	20921	144	15.	90.28	53.

#### 5.4 Flexural test experiment

There is a wide variety of test methods available for flexure testing described (ASTM: D7264) addressing the particular needs of heterogeneous non-isotropic materials. In general, flexure test type tests are applicable to quality control and material selection where comparative rather than absolute values are required. Flexural properties of the laminates were determined using the standard three point bending test method. For flexure

test, there is no involvement of end-tabs or changes in the laminate shape. Tests can be conducted on simply supported beams of constant cross-sectional area. A schematic of simply supported beam at close to ends flat rectangular laminate is shown in Figure-14(a). The laminate is centrally loaded representing three-point bending test. Dimensions of the three laminates with cross-sectional areas having constant width but different thicknesses are shown in Figure-14(b).

**Figure-14.** Schematics: a) laminate bending and b) cross-sectional area.

Approximate dimensions and relevant simple support of span to depth ratios provides base to

formulation the calculation of Young's modulus from the load-displacement relation given in Table-9.

**Table-9.** Formulation used to calculate young's modulus.

Bending moment	Moment of area	Max bending stress	Load	Young's modulus
$M = P \frac{L}{4}$	$I = \frac{wt^3}{12}$	$\sigma_{max} = \frac{M \left( \frac{t}{2} \right)}{I} = \frac{3 PL}{2 wt^2}$	$P = \frac{3 \sigma wt^2}{2 L}$	$E = \frac{PL^3}{48I\delta}$

The machine shown in Figure-13 is used with changed testing chamber. Two laminates from the three types of laminates were selected and atypical one is shown in Figure-15(a) with test chamber in (b). The laminates were placed in the fixture and gradually loaded. The laminates were held in place in the machine in flexural test chamber and gradually loaded. During flexural tests all of the laminates experienced deflection under increased

loading. The deflection typically occurred at the middle of the laminates, which was in contact with the machine head, therefore considered to be a loaded edge. The loading produces the maximum bending moment and maximum stress under the loading nose. The vertical load could deflect (bend) the laminate and even fracture the outer fibres of the laminate under excessive loading.

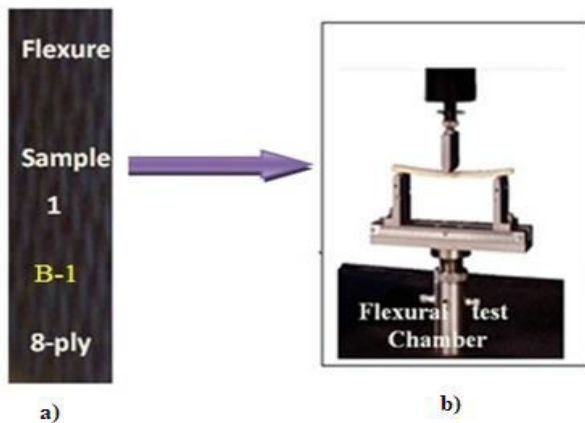


**Figure-15.** a) Test laminate b) test chamber of INSTRON™ 5585H.

The strain values and the other data were recorded by software installed on the data acquisition system at specified load increments so that the curve is plotted for each laminate. In the beginning of the bending test the load-deflection curves show slightly erratic behaviour, but along the course of the curves there is a definable linear portion. Independent tests for every laminate were carried out and mean moduli were calculated for the every laminate. Measurements of the strain values, deflections and loads were used to determine the Young's modulus.

As shown in Table-10 below the recorded voltage range was scaled by gain factor and strains values were calculated. Stresses were calculated from the recorded applied load divided by the corresponding cross-sectional area. Young's moduli were then calculated using the strain and stress values and have been shown in column 8 of Table-10.

**Table-10.** Flexural test results.

Test	Laminate	Bridge factor	Micro-strain	Load N	Stress GPa	Elastic modulus GPa
B-1	8-Ply	0.4	440.	20	26.04	52.1
B-2		0.39	429.	20	26.04	50.2
B-3	16-Ply	0.52	572.	80	26.04	45.5
B-4		0.5	550.	80	26.04	45.28
B-5	24-Ply	0.54	594.	170	24.59	41.35
B-6		0.53	583.	170	24.6	41.13

### 5.5 Overall comparison of approximated elastic moduli

Selected young's moduli for all the 8-, 16, and 24-Ply laminates obtained from simulation, rule of mixture, Hart Smith, tensile, and flexural testing methodologies are compared in Table-11. Good agreement

of the predicted values of Young's moduli for every laminate was found. The comparisons confirmed that results of the mechanical properties (physical plus elastic stiffness) delivered from the MATLAB™ programs are reliable.

**Table-11.** Comparison of Young's moduli from different methods.

Laminate	Methodologies applied				
	Simulation	Rule of mixture	Hart Smith	Tensile	Flexural
	Young's modulus GPa				
8-Ply	56	58.5	40.4	45.6	52
16-Ply	48.6	58.6	40.1	46.7	45
24-Ply	45.8	58.8	40.	52.2	41

## 6. CONCLUSIONS

In this investigation, engineering properties of quasi-isotropic 8-, 16-, and 24-Ply carbon fibre-reinforced laminated composite panels were determined applying simulation methodology based on micro-macro mechanics of the laminates. Physical properties were determined and ignition loss tests were conducted to evaluate volume fractions quantities from the rule of mixture. The rule of mixture and inverse rule of mixture were utilised to approximate engineering constants. Then two-dimensional

stress-strain relation and micro-macro mechanics methods were applied to formulate lamina, angle lamina, and three-dimensional laminate elements. Computer codes were developed to determine range of the engineering constants. Selected data obtained from the simulations were verified with tensile and flexural physical testing. Based on comparison of the results the following conclusions can be extracted:



- Micro-macro mechanics of a lamina were utilised to approximate effective elastic constants for three-dimensional laminates.
- Simulation produced results were validated against the values obtained by volume fractions and Hart Smith rules, tensile, and flexural testing and were found to be within acceptable range with ( $\pm 10\%$ ) deviations.
- Elastic constants determined from MATLAB™ simulations were also compared to the intra-simulation values as a function of fibre rotations and were found to be in good agreement.

Based on comparisons of the results it is proposed that three-dimensional (full range) of effective elastic constants can be efficiently determined from information of the volume fraction, two-dimensional micro-mechanics laws, and computer simulations with reduced physical testing.

## REFERENCES

- [1] Morgan P. 2005. Carbon Fibres and their composites. Taylor & Francis, Boca Raton, USA.
- [2] Yang B, Kozey V, Adanur S, Kumar S. 2000. Bending, compression, and shear behaviour of woven glass fibre- epoxy composites. Composites: Part B. 31: 715-21.
- [3] Hussain SA, Reddy SB and V, and Reddy VN. 2008. Prediction of elastic properties of FRP composite lamina for longitudinal loading. Asian Research Publishing Network. 3(6): 70-75.
- [4] Gao XL, Li K, and Mall S. 2003. A mechanics-of-materials model for predicting Young's modulus of damaged woven fabric composites, involving three damage modes, Int J Solids Struct. 40: 981-999.
- [5] John EL, XiaowenY, Mark II. 2012. Characterisation of voids in fibre reinforced composite materials. NDT&E International. 46: 122-127.
- [6] Keshavamurthy YC, Nanjundaradhya NV, Ramesh SS, Kulkarni RS. 2012. Investigation of tensile properties of fibre reinforced angle ply laminated composites. Int. J Emerg Technol Adv Eng. 2(4): 700-703.
- [7] Emilia S, Nicolai B and Paul B. 2001. Mechanical characteristics of composite materials obtained by different technologies. Academic J Manufactur Eng. 9(3): 100-105.
- [8] Altaf HS, PandurangaduV, Amba PRG. 2013. Prediction of elastic constants of carbon T300/ epoxy composite using soft computing. Int J Inn Research in Sci Eng Technol. 2(7): 2762-2770.
- [9] Bradley LR, Bowen CR, McEnaney B, Johnson LR. 2007. Shear properties of a carbon/carbon composite with non-woven felt and continuous fibre reinforcement layers. Carbon. 45: 2178-2187.
- [10] Mujika F. 2006. On the difference between flexural moduli obtained by three-point and four-point bending tests. Poly Testing. 25: 214-220.
- [11] Satish KG, Siddeswarappa B, Mohamed KK. 2010. Characterization of in-plane mechanical properties of laminated hybrid composites. J Miner Mater Character Eng. 9(2): 105-114.
- [12] Irina P, Cristina M, Constant I. 2013. The determination of Young modulus for cfrp using three point bending tests at different span lengths. Scientific Bulletin-University Politehnica of Bucharest. 75: 121-128.
- [13] Konrad Gliesche, Tamara Hubner, Holger Orawetz. 2005. Investigations of in-plane shear properties of  $\pm 45^\circ$  carbon/epoxy composites using tensile testing and optical deformation analysis. Compos Sci Technol. 65: 163-171.
- [14] Bradley LR. 2003. Mechanical testing and modelling of carbon-carbon composites for aircraft disc brakes. PhD thesis, University of Bath, UK.
- [15] Barbero EJ. 2010. Introduction to composite materials design, (Second Edition), CRC Press Taylor & Francis Group.
- [16] D. Bhagwan, Agarwal and Lawrence J. 2012. Broutman, Analysis and Performance of Fibre Composites. John Wiley and Sons Inc, Unites States.
- [17] Romano F., Fiori J., Mercurio U. May 2009. Structural Design and Test Capability of a CFRP Aileron. Composite Structures. 88(3): 333-341.
- [18] Liyong Tong, Adrian P. Mouritz and Michael K. 2002. Bannister '3D Fibre Reinforced Polymer Composites' Book, Elsevier Science Ltd. All Rights Reserved.



- [19] Prashanth Banakar<sup>1</sup>, H.K. Shivananda<sup>2</sup> and H.B. Niranjana<sup>3</sup>. 2012. Influence of Fibre Orientation and Thickness on Tensile Properties of Laminated Polymer Composites. *Int. J. Pure Appl. Sci. Technol.* 9(1): 61-68.
- [20] F. Mujika. 2006. On the difference between flexural moduli obtained by three-point and four-point bending tests, *Polymer Testing*. 25: 214-220.
- [21] F. Gibson. 2007. Principles of composite materials mechanics. Taylor & Francis Group, CRC Press Boca Raton. pp. 83-126.